JOURNAL OF Materials CHEMISTRY

Structural phase transition in quasi-one-dimensional conductors $(BDTFP)_2X(PhCl)_{0.5}$ (X = PF_6 and AsF_6) [BDTFP = 5,7-bis(1,3-dithiol-2-ylidene)-5,7-dihydrofuro[3,4-*b*]pyrazine; PhCl = chlorobenzene]

M. Uruichi,*[a] K. Yakushi,[a] T. Shirahata,[b] K. Takahashi,[c] T. Mori[d] and T. Nakamura[a]

[a]*Institute for Molecular Science, Myodaiji 444-8585, Japan. E-mail: uruichi@ims.ac.jp*
[b]*Department of Chemistry, Tohoku University, Sendai 980-8578, Japan*
[c]*Center for Interdisciplinary Research, Tohoku University, Sendai 980-8578, Japan*
[d]*Tokyo Institute of Technology, Ookayama, Tokyo 152-8552, Japan*

Received 4th March 2002, Accepted 30th May 2002
First published as an Advance Article on the web 15th July 2002

We present the low-temperature crystal structures of $(BDTFP)_2PF_6$ and $(BDTFP)_2AsF_6$ below the phase transition temperatures (T_p). In the former compound, the *c*-axis is doubled, and the dimerized structure is therefore changed into a tetramerized structure. At the same time, a new charge-transfer transition appears at *ca.* 7000–8000 cm^{-1}. These two findings are consistent with the non-magnetic state below T_p. In the latter compound, on the other hand, the dimerized structure is maintained below T_p, and the AsF_6 ion rotates along with the *ca.* 10° rotation of BDTFP. This structural change is the origin of the first-order phase transition to a paramagnetic state.

Introduction

BDTFP {5,7-bis(1,3-dithiol-2-ylidene)-5,7-dihydrofuro[3,4-*b*]-pyrazine} is a new electron donor molecule synthesized by a group at Tohoku University (Scheme 1).[1] Ise *et al.* characterized the crystal structures of the charge transfer (CT) salts $(BDTFP)_2X(PhCl)_{0.5}$ (X = PF_6, AsF_6; PhCl = chlorobenzene) and claimed that these CT salts can be regarded as a two-leg ladder system, based on the calculation of the overlap integrals. BDTFP molecules are stacked along the *c*-axis, and have a dimerized structure with an overlap integral ratio of $c2/c1 = 0.5$ (Fig. 1). The unit cell involves two molecular stacks, between which a comparable overlap integral ($p/c1 = 0.3$) (Fig. 1) is found. If we consider the dimer as a super-molecule, this compound can be regarded as a two-leg spin-ladder system. One of the purposes of this study is to examine the inter-chain interaction by observing an optical transition polarized along a rung of the ladder.

Both CT salts are non-metallic and have a small activation energy ($E_a \approx 0.08$ eV), and they undergo phase transitions from a low-resistivity phase to a high-resistivity phase at 175 and 220 K for X = PF_6 and AsF_6, respectively.[1,2] Nakamura *et al.* studied these compounds by the use of EPR, and found that their phase transitions occur at different temperatures.[3] The PF_6 salt undergoes a spin-singlet transition at 175 K, whereas the AsF_6 salt shows a first-order phase transition to a paramagnetic state with a small spin-gap nature at 230 K, then undergoes a transition to an anti-ferromagnetic state below 14 K. In the heating process, the first phase transition occurs at 280 K with a large hysteresis. In this sense, the nature of the phase transition is quite different between these compounds, although they are isostructural at room temperature. Another aim of this study is to reveal the structural change below the phase transition, which seems to be different between PF_6 and AsF_6 salts.

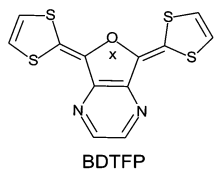

BDTFP

Scheme 1 Structural formula of BDTFP. The mark x shows the center of the HOMO.

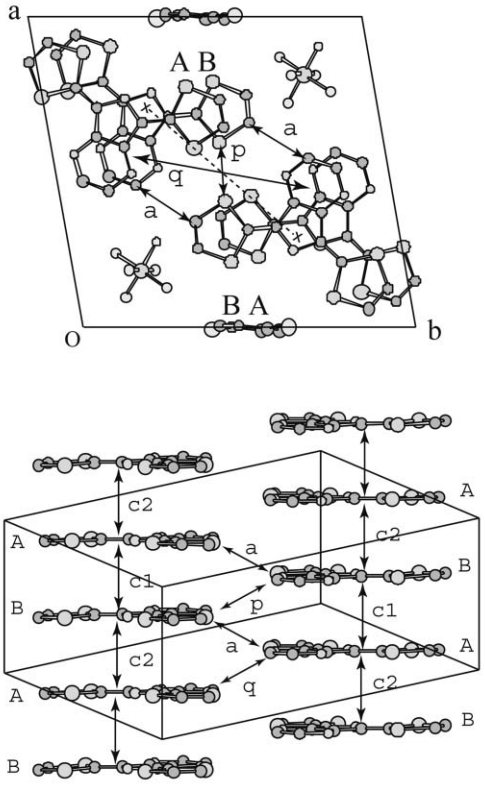

Fig. 1 Top (upper) and side (lower) views of the molecular stacks of BDTFP in $(BDTFP)_2PF_6(PhCl)_{0.5}$ at room temperature. The unit cell involves four molecules, two (A and B) of which are crystallographically independent. The definition of transfer integrals is shown. X denotes the center of the HOMO of BDTFP.

 DOI: 10.1039/b202259c

Experimental

The single crystals were grown using the method described by Ise *et al.*[1] The crystal shapes are thin and needle-like, developing mostly along the *c*-axis with the development of the *bc* crystal face. The absorption spectrum in solution was measured on a HITACHI U-3500. A standard 10 mm-long cell was used for the measurement of the neutral BDTFP molecule and AsF_6 salt. The polarized reflection spectrum was obtained using two spectrometers and a microscope (Spectratech IR-Plan). A Nicolet Magna 760 FT-IR spectrometer was used for the 600–12 000 cm^{-1} region, and an Atago Macs320 multi-channel detection system was used for the 11 000–30 000 cm^{-1} region. For the low-temperature experiment, a small goniometer head was attached to the cold head of the cryostat (Oxford CF1104s) fixed on an XYZ stage. The details of the experimental method have been described previously.[4] The crystal face was determined by the X-ray diffraction method using a Rigaku AFC-7R-2 four-circle diffractometer. The X-ray diffraction experiment at low temperature was conducted using an imaging-plate detection system (Rigaku R-AXIS-4). The sample temperature was lowered using liquid nitrogen. The temperature sensor was set at the nozzle, 8 mm from the sample.

CCDC reference numbers 181035–181038.

See http://www.rsc.org/suppdata/jm/b2/b202259c/ for crystallographic data in CIF or other electronic format.

Results and discussion

Table 1 shows the lattice parameters of the type 1 PF_6 salt at room temperature and 90 K, the type 2 PF_6 salt at room temperature, and the type 1 AsF_6 salt at room temperature and 100 K. As will be described in the final section, we have found three types of charge-transfer salts in PF_6 salts and two types in the AsF_6 salt. We first discuss the type 1 crystals, the physical properties of which are studied most.

Room-temperature reflection spectrum

Fig. 1 shows the top and side views of the crystal structure of the PF_6 salt. The unit cell contains two molecular stacks running along the *c*-axis. Inter-stack interaction is allowed only between these two stacks; these two stacks are blocked from other stacks by the counter-anion PF_6 and the solvent molecule chlorobenzene. The largest inter-stack overlap integral is *p*, between the B molecules. The polarization direction of the CT band is given by the direction connecting the centers of the HOMOs (highest occupied molecular orbitals). The center of the HOMO is calculated using the following equation:

$$r_0 = \sum_{i=1}^{N} c_i^2 r_i$$

where c_i is the coefficient of the p_z atomic orbital of the *i*-th site in the HOMO, which is calculated by extended Hückel approximation. Owing to the C_{2v} symmetry of BDTFP, the center of the HOMO is located on the axis of two-fold rotation, which is marked as **x** in Scheme 1. The angle between the direction connecting the centers of molecules and the polarization direction of the light [$E \perp c$ on (100)] is calculated to be $\theta = 39^\circ$. Reflection spectra polarized parallel and perpendicular to the *c*-axis on the (100) crystal face are presented in Fig. 2. As shown in this figure, the CT band appears only along the *c* direction in both compounds. If an inter-stack CT band has sufficient intensity along the direction shown by the broken line in Fig. 1, the intensity is reduced to $\cos^2\theta = 0.6$ in the $E \perp c$ spectrum. Since no dispersion is found in the $E \perp c$ reflectivity spectrum up to 8000 cm^{-1}, we consider that the inter-stack interaction is much smaller than what is predicted by the calculation of the overlap integral. Thus, we regard each compound as a three-quarter-filled quasi-one-dimensional system. To assign the dispersion at 10 000 cm^{-1} in the $E \perp c$ spectrum of the AsF_6 salt, we compared the $E \perp c$ conductivity spectrum with the solution spectra of $BDTFP^0$ and $BDTFP^+$, as shown in Fig. 3.[5] It is obvious that the 10 000 cm^{-1} band is assigned to the electronic local excitation of $BDTFP^+$, which is polarized perpendicular to the mirror plane of the molecule. The corresponding dispersion is not so clear in the $E \perp c$ spectrum of the

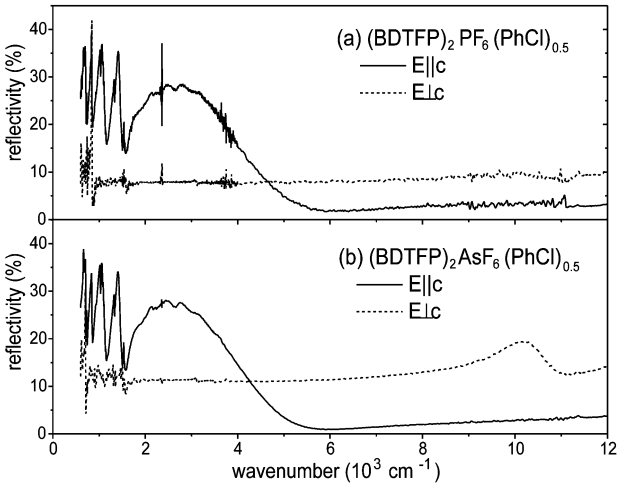

Fig. 2 Room-temperature polarized reflection spectra of (a) $(BDTFP)_2PF_6(PhCl)_{0.5}$ and (b) $(BDTFP)_2AsF_6(PhCl)_{0.5}$.

Table 1 Lattice parameters of PF_6 and AsF_6 salts of BDTFP

	PF_6			AsF_6	
	Type 1		Type 2	Type 1	
Temperature	RT[a]	90 K	RT	RT[a]	100 K
Space group	$P\bar{1}$	$P\bar{1}$	$P\bar{1}$	$P\bar{1}$	$P\bar{1}$
a/Å	15.438(5)	15.159(4)	14.90(1)	15.628(3)	15.252(4)
b/Å	16.147(2)	16.159(3)	16.077(3)	16.285(7)	16.083(5)
c/Å	6.981(1)	13.749(2)	10.740(4)	6.969(1)	6.890(1)
α/°	100.91(1)	103.59(1)	92.69(3)	100.28(2)	100.22(2)
β/°	101.81(2)	99.92(2)	83.78(5)	102.86(1)	98.09(2)
γ/°	97.25(2)	78.70(2)	99.45(5)	97.13(3)	100.55(2)
V/Å^3	1647.7(6)	3182(1)	2521(2)	1676.4(8)	1608.8(7)
R-factor	0.047	0.051		0.076	0.065

[a]The hydrogen atom at the position *para* to the chlorine atom in chlorobenzene is not included in the least-squares calculation, because the chlorobenzene is located on the center of symmetry and is thus disordered.

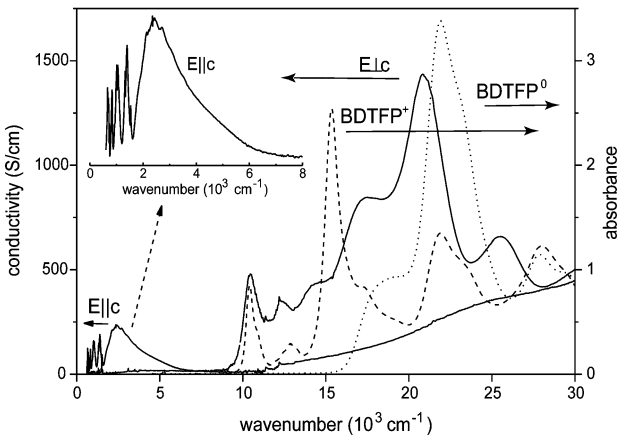

Fig. 3 Room-temperature optical conductivity spectra of $(BDTFP)_2AsF_6(PhCl)_{0.5}$ for $E\|c$ (solid line) and $E\perp c$ (solid line). The solution spectra of BDTFP and the AsF_6 salt are drawn by dotted and broken lines, respectively. The inset shows the infrared and near-infrared region of the $E\|c$ spectrum on an expanded scale.

PF_6 salt, although we carefully examined the polarization direction in this crystal. The polarization direction of the first local excitation of the PF_6 salt seems to be rotated in the direction parallel to the mirror axis of BDTFP.

Let us discuss the infrared reflectivity of $E\|c$. As shown in Fig. 2, the reflectivities of the PF_6 and AsF_6 salts are almost the same with regard to each other. The $E\|c$ optical conductivity $\sigma(\omega)$ of the AsF_6 salt is shown in the inset of Fig. 3. The sharp bands below 1800 cm^{-1} are the vibronic bands, the intensity of which is enhanced through the EMV (electron-molecular-vibration) coupling.[6,7] The appearance of the strong vibronic band is consistent with the dimerized stack structure.[8,9] The intensity of the vibronic structure is almost the same between the PF_6 and AsF_6 salts, which suggests that their dimerization amplitudes are comparable. The optical conductivity has a peak at around 2400 cm^{-1} (0.3 eV) and no Drude term, which is consistent with the resistivity experiment that provides activation energies of 0.078 eV for the AsF_6 salt and 0.076 eV for the PF_6 salt. Above the phase transition temperature, the resemblance of their reflectivities and activation energies suggests that the parameters (Coulomb interaction and dimerization amplitude) to determine the electronic structure of these systems are very similar. The theory of the optical transition and electron excitation of a quarter-filled dimerized system such as $(TMTTF)_2X$ (TMTTF = tetramethyltetrathiafulvalene) has been studied by Favand and Mila.[10] When the dimerization is strong, as it is in these compounds, the system takes a non-metallic state, and the charge gap ($2E_a$) is nearly the same as the lowest optical transition (absorption edge). According to their numerical calculation, the absorption edge is close to $2(t_1 - t_2)$, when $U/t_1 > 5$, where t_1 and t_2 are the intra- and inter-dimer transfer integrals, respectively, and U is the on-site Coulomb energy. Since it is difficult to determine the absorption edge in the $\sigma(\omega)$ spectrum, we take twice the activation energy as a charge gap, then estimate $2(t_1 - t_2)$ as *ca.* 0.16 eV. On the other hand, the average transfer integral $(t_1 + t_2)/2$ is roughly estimated from the plasma frequency ω_p, which is defined by the following equation:

$$\omega_p^2 = \frac{2}{\varepsilon_0 \pi} \int_0^{\omega_0} \sigma(\omega)\, d\omega$$

where ε_0 is the dielectric constant of a vacuum. When we take the cut-off frequency ω_0 as 8000 cm^{-1}, the plasma frequency is numerically obtained as 5000 cm^{-1}. If we adopt a simple one-dimensional tight-binding model,[9] the transfer integral is roughly estimated as $(t_1 + t_2)/2 \approx 0.08$ eV.[11] Combining two relations, t_1 and t_2 are estimated as *ca.* 0.12 and *ca.* 0.04 eV, respectively.

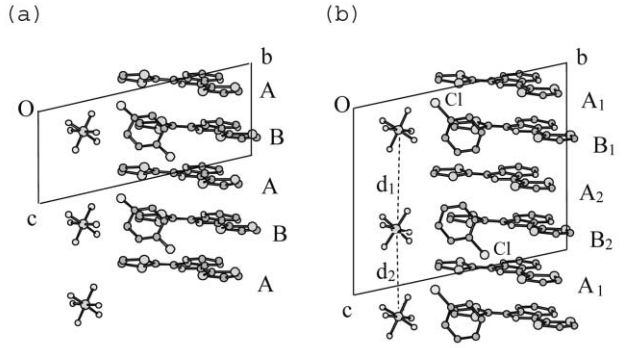

Fig. 4 Side view of the molecular column in $(BDTFP)_2PF_6(PhCl)_{0.5}$ at (a) room temperature and (b) 90 K. The unit cell is doubled along the c-axis at 90 K, and the anion–anion separation becomes non-equivalent in such a way as $d_1 = 7.21$ and $d_2 = 6.51$ Å.

The ratio t_2/t_1 is comparable with the ratio of the overlap integrals $c2/c1 \approx 0.5$.

Low-temperature phase of the PF_6 salt

Below the phase transition temperature ($T_p = 175$ K), the spin susceptibility vanishes, which indicates the formation of a spin-singlet state.[3] Strong diffraction spots for a $\boldsymbol{q} = (0, 0, 1/2)$ super-lattice are clearly observed below T_p. Fig. 4 shows a comparison of the stacking patterns viewed along the a-axis at room temperature and 90 K. Since the c-axis is doubled at 90 K, BDTFP forms a tetramerized structure with four non-equivalent sites, A_1, B_1, A_2 and B_2, and the anion–anion distance also becomes non-uniform as shown by d_1 and d_2 in Fig. 4. The inter-anion distance changes from $d = 6.981$ Å to $d_1 = 7.21$ Å and $d_2 = 6.51$ Å. Furthermore, the disordered chlorobenzene at room temperature is ordered at 90 K (see the position of Cl of the PhCl). The counter-anion PF_6 does not change the orientation. This low-temperature structure is consistent with the spin-singlet state, since a repeating unit involves paired electrons. To see the stacking pattern, or, in other words, the BOW (bond order wave) pattern, we calculated the overlap integrals, which are 8.80×10^{-3} for B_2A_1, 11.5×10^{-3} for A_1B_1, 8.25×10^{-3} for B_1A_2, and 1.02×10^{-3} for A_2B_2. Thus, $B_2A_1B_1A_2$ is regarded as the unit of the tetramer, and the BOW pattern is schematically presented as $A_2\cdots B_2{-}A_1{=}B_1{-}A_2\cdots B_2$.

Fig. 5 shows the $E\|c$ reflection spectra at room temperature and 16 K. A significant feature at low temperature is the appearance of the new electronic transition at 7500 cm^{-1} (shown by a thick arrow). Since this new band is polarized along the stacking axis, this absorption band is also assigned to the CT transition within the stack. We name these two CT transitions as CT_L, for the 2400 cm^{-1} band, and CT_H, for the 7500 cm^{-1} band. Since the excitation energy of CT_H is much larger than that of CT_L, we interpret the CT_H excited state as involving two holes in one site. In this case, the excitation energy is lifted up by the effect of an on-site Coulomb energy U. The interpretation of CT_L and CT_H is schematically drawn in the inset of Fig. 5. The CT_H band is observable only when the two holes are distributed at neighboring sites. This means that a significant change occurs in the distribution of charge above and below T_p. Above T_p, the holes are distributed equally (+0.5) within a dimer or alternately distributed as $[0 + \delta, 1 - \delta, 0 + \delta, 1 - \delta]$ (δ is a fractional charge), because the repeating unit is two molecules. On the other hand, below T_p, the holes seem to be distributed as $[0 + \delta, 1 - \delta, 1 - \delta, 0 + \delta]$ in the tetrameric unit. Comparing this hole-distribution (CDW) pattern with the low-temperature structure, we infer that A_1 and B_1 are charge-rich and that A_2 and B_2 are charge-poor, because A_1 and B_1 are closer to PF_6^- and an electron-accepting chlorine atom in chlorobenzene. Then our model for the

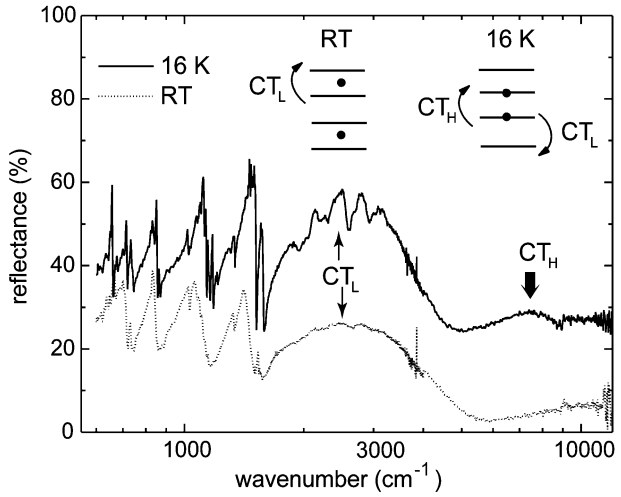

Fig. 5 Reflection spectrum ($E\|c$) of $(BDTFP)_2PF_6(PhCl)_{0.5}$ at 16 K (solid line) and room temperature (dotted line). The inset shows the schematic configuration of holes in a dimer (RT) and tetramer (16 K). CT_H involves an electronic configuration in which the HOMO is doubly occupied, while CT_L does not involve such a configuration. Note that a new CT transition (CT_H) appears at 16 K.

BOW and CDW patterns is schematically represented as $\cdots B_2^{\delta}$–$A_1^{1-\delta}$=$B_1^{1-\delta}$–$A_2^{\delta}\cdots$, which corresponds to $2k_F$ BOW + $2k_F$ CDW according to the classification by Mazumdar *et al.*[12] This model is consistent with the appearance of the CT_H band, which is associated with the charge transfer that occurs between A_1 and B_1 with the largest the overlap integral. If the molecule has a charge-sensitive vibrational mode, the frequency of which shifts depending upon the charge on a molecule, such a vibrational mode splits into two when the charge is separated into $0 + \delta$ and $1 - \delta$. However, we could not confirm this sort of splitting below T_p. BDTFP seems to have no charge-sensitive vibrational mode, because the Raman spectrum of $BDTFP^0$ in the C=C stretching region is very similar to that of $BDTFP^{0.5+}$. The analogous charge separation or the reorganization of the hole distribution has been found in $(EDO\text{-}TTF)_2PF_6$ (EDO-TTF = ethylenedioxytetrathiafulvalene) in a more typical manner, in which δ is nearly equal to zero, and not only is the CT_H band observed, but the splitting of the C=C stretching modes is also found.[13]

Low-temperature phase of the AsF_6 salt

The crystal structure of the AsF_6 salt is isostructural with that of the PF_6 salt, as shown in Fig. 6(a) (see also the top view in Fig. 1). According to the EPR experiment by Nakamura *et al.*, the spin susceptibility of the AsF_6 salt behaves very differently from that of the PF_6 salt. On lowering the temperature, the spin susceptibility shows a first order phase transition at $T_p = 230$ K with a hysteresis of *ca.* 50 K.[3] Below T_p, the spin–spin interaction is weakened in contrast to the case of the PF_6 salt. The electronic excitation (CT_L) in the low-frequency region (< 5000 cm^{-1}) of the $E\|c$ reflection spectra measured at 150 and 12 K are similar to the 16 K spectrum of the PF_6 salt. However, the 7500 cm^{-1} band is not found at 150 K or at 12 K in the AsF_6 salt. In correspondence with the spectral characteristics, the crystal structure at 100 K does not show the doubling of the *c*-axis. However, we found at 100 K that this compound changed the molecular arrangement. As shown in Fig. 6(b), the counter-anion AsF_6 rotates about 90° around the *c*-axis. At the same time, BDTFP rotates the molecular plane by *ca.* 10° nearly around the *b* axis. At room temperature, the molecular plane is almost perpendicular to the *c*-axis (stacking axis), whereas at 100 K, the normal of the molecular plane is tilted against the *c*-axis as shown in Fig. 7. PhCl is more disordered at 100 K than at room temperature. The calculation of the overlap integral based on this structural change suggests that the inter-dimer interaction at 100 K reduced to 60% of that at room temperature. Thus, the spin–spin interaction is expected to be weaker. This structural change is consistent with the abrupt increase of the spin susceptibility at T_p and the Curie-like behavior below T_p. The phase transition from $4k_F$ BOW to $2k_F$ BOW found in the PF_6 salt is often observed in a one-dimensional system.[14] However, the phase transition found in the AsF_6 salt is rare. The origin of this phase transition is interesting, but at the moment unclear.

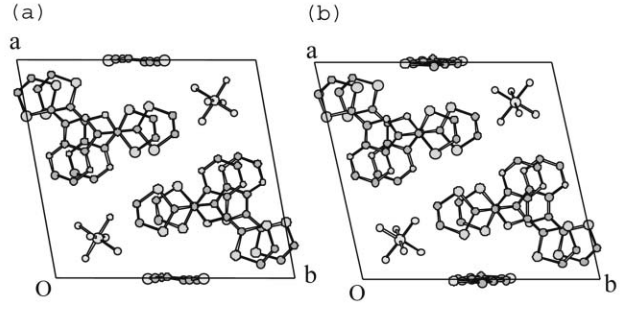

Fig. 6 Top view of the molecular stack of $(BDTFP)_2AsF_6(PhCl)_{0.5}$: (a) above (RT), and (b) below (100 K) T_p. Note that AsF_6 ions rotate by about 90° around the *c*-axis.

Polymorphism

At least three different types of crystals were found in the PF_6 salts. Fig. 8 shows the $E\|c$ optical conductivity spectra of the three types in the infrared and near-infrared regions. We have described the optical and structural characteristics above and below T_p of type 1, which exhibits a sharp phase transition. The optical spectrum of type 2 is quite different from that of type 1: the position of CT_L in type 2 is significantly higher than that of type 1, and CT_H (at 8000 cm^{-1}) has already appeared at room temperature. This compound shows no EPR signal in a whole temperature range, and is presumed to have low conductivity, since the optical gap is clearly observed around 2000 cm^{-1}, as shown in this figure. As shown in Table 1, the *c*-axis is about 1.5 times as large as that of the type 1 crystal, which suggests that the stack of BDTFP consists of a trimer. Since the EPR signal is silent, we speculate that this compound has a 3 : 2 chemical composition with a counter-anion. Actually, the preliminary crystal structure analysis is consistent with this speculation, although full analysis was unsuccessful due to the quality of the crystal. The 3 : 2 chemical ratio is consistent with the appearance of CT_H. As shown in Fig. 8, the low-frequency optical spectrum of type 3 more closely resembles that of type 1 than that of type 2, but CT_H is already observed at room temperature. In the type 2 crystal, the two strong vibronic bands, at 1182 and 1443 cm^{-1}, are superimposed on the vibronic bands

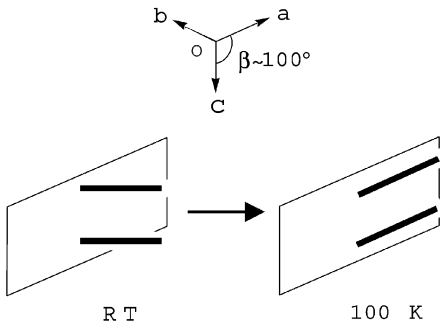

Fig. 7 Schematic drawing to show the tilting of the BDTFP molecular planes from room temperature (RT) to 100 K. The molecular planes nearly perpendicular to the *c*-axis at RT are tilted by *ca.* 10° at 100 K.

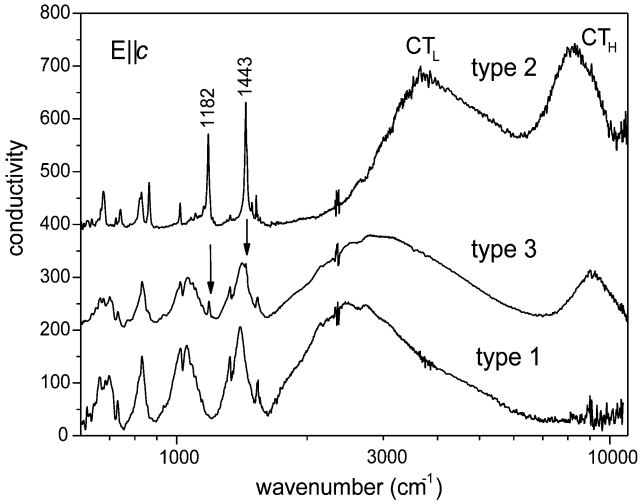

Fig. 8 Optical conductivity spectra of type 1, 2, and 3 crystals of the PF_6 salts of BDTFP measured at room temperature.

of type 1 as indicated by the arrows in Fig. 8. The intensities of these two vibronic bands change depending upon the crystals. The type 3 crystal appears to be a mixture of type 1 and type 2, in which the molecular stacks are running in the same direction. However, the lattice constants are almost the same as those of type 1, and diffraction spots coming from the type 2 crystal cannot be found in the imaging plate. The type 3 crystal shows a phase transition in magnetic susceptibility near the same temperature as type 1 does, but the drop in susceptibility of type 3 is not sharp. Therefore, we think that type 3 is not a simple mixture of type 1 and type 2.

The type 3 crystals are also found in the AsF_6 salt, though the type 2 has not been found. The optical spectrum of the type 3 AsF_6 salt is almost the same as that of the type 3 PF_6 salt. This crystal shows the additional two strong vibronic bands and CT_H. The magnetic susceptibility of the type 3 AsF_6 salt shows no first-order phase transition at around 250 K but shows an incomplete drop in magnetic susceptibility at around 130 K. The paramagnetic susceptibility remains, in addition to a large amount of Curie component (*ca.* 6–7%), below T_p.

Acknowledgements

This research was supported in part by a Grant-in-Aid for Scientific Research on Priority Areas (B) of Molecular Conductors and Magnets (Area No. 730/Grant No.11224212) from the Ministry of Education, Science, Sports, and Culture of Japan.

References

1 T. Ise, T. Mori and K. Takahashi, *J. Mater. Chem.*, 2001, **11**, 264.
2 The transition temperature in resistivity given by Ise *et al.*[1] is lower than that in spin susceptibility given by Nakamura *et al.*[3] This may be associated with the large hysteresis of this first-order phase transition.
3 T. Nakamura, T. Ise, K. Takahashi, M. Uruichi, K. Yakushi and T. Mori, *Mol. Cryst. Liq. Cryst.*, in press.
4 M. Uruichi, K. Yakushi and Y. Yamashita, *J. Phys. Soc. Jpn.*, 1999, **68**, 531.
5 The optical conductivity spectrum is obtained through Kramers–Kronig transformation.
6 M. J. Rice, N. O. Lipari and S. Strässler, *Phys. Rev. Lett.*, 1977, **39**, 1359.
7 M. J. Rice, *Solid State Commun.*, 1979, **31**, 93.
8 M. Uruichi, K. Yakushi and Y. Yamashita, *J. Phys. Soc. Jpn.*, 1999, **68**, 531.
9 M. Uruichi, Y. Yamashita and K. Yakushi, *J. Mater. Chem.*, 2000, **10**, 2716.
10 J. Favand and F. Mila, *Phys. Rev. Sect. B*, 1996, **54**, 110425.
11 Strictly speaking, the relation between plasma frequency and transfer integral holds only in the case of a one-dimensional metal. However, the plasma frequency obtained by numerical integration of conductivity is nearly equal to that of a metallic system.
12 S. Mazumdar, S. Ramasesha, R. T. Clay and D. K. Compbell, *Phys. Rev. Lett.*, 1999, **82**, 1522.
13 O. Drozdova, K. Yakushi, A. Ota, H. Yamochi and G. Saito, *Proceedings of Yamada Conference LVI*, to be published in *Synth. Met*.
14 B. van Bodegom, B. C. Larson and H. A. Mock, *Phys. Rev. Sect. B*, 1981, **24**, 1520.